

# **“Design and Optimisation of Cathodic Protection Systems Using Computer Simulation”**

Robert A Adey, John Baynham

*Computational Mechanics BEASY, Ashurst Lodge, Southampton, Hampshire, SO40 7AA, UK*

*Email: [r.adey@beasy.com](mailto:r.adey@beasy.com)*

## **ABSTRACT**

The design of cathodic protection systems normally relies on a combination of experience, experimental data and heuristics. However, problems and failures of CP systems not only has an economic cost, it can also present a threat to life and the environment.

This paper will describe the application of a software system designed to simulate the performance of cathodic protection systems and predict the impact of the design parameters and the environment on its performance. Two applications are presented. The first describes an approach to the global optimisation of a ship's Impressed Current Cathodic Protection (ICCP) system using the boundary element method coupled with “Simulated Annealing” (SA) algorithm and search methods. In the second the modelling and optimisation of a CP systems for storage tanks is described including the impact of coating holidays and stray currents.

## **INTRODUCTION**

Cathodic protection has been widely used for protecting structures from corrosion. The design of the cathodic protection systems, either sacrificial anode cathodic protection (CP) or impressed current cathodic protection (ICCP) system, require the solution of the Laplace's or Poisson's equation with the relevant boundary conditions to give the current and potential distribution in the solution domain. Even for relatively simple geometry, analytical solutions are usually not possible. Various numerical approaches have therefore been adopted and the Boundary Element Method has been found to be the most proficient numerical method for the modelling of ship's cathodic protection system [1 - 4].

The design goal of an ICCP system is to produce an evenly distributed protection potential on the structure as well as to reduce the power consumption of the anodes to a minimum. The available design variables are the number of anodes (and their location) and the location of the reference cells. The constraints on the design are the values of the potential on the structure. In order to provide adequate protection the potential must be less than a specified value (e.g., -800mv). In order to prevent over protection the potential must be greater than a specified value (e.g., -900mv). By combining an automatic optimisation procedure with the BEM model of the ICCP system an optimum solution can be obtained.

To achieve the design goals the BEM model has been coupled with a ‘‘Simulated Annealing’’ (SA) algorithm and search method. The SA algorithm is able to deal with both continuous and discretised variables and was used to identify the global minimum. The direct search method was used to find the actual minimum efficiently.

## The Boundary Element Model

The governing equation in the bounded uniform seawater medium is:

$$k\nabla^2 u = 0 \quad (1)$$

with the boundary condition in the solution domain is defined by:

$$\Gamma = \Gamma_A + \Gamma_C + \Gamma_I \quad (2)$$

Where  $u$  is the electric potential,  $\Gamma_A$  is the anodic surface,  $\Gamma_C$  is the cathodic surface and  $\Gamma_I$  is the insulated surface.

The boundary element method formulation in electro-potential, Green's theorem applied to Laplace's equation is formulated as [1]:

$$\int_{\Omega} u(\nabla^2 u^*) d\Omega = \int_{\Gamma} (q^* u - u^* q) d\Gamma \quad (3)$$

Introducing elements into equation (3), after transformation of variables,

$$c_i u_i = \sum_{j=1}^N \int_{\Gamma_j} (u^* q - u q^*) d\Gamma_j \quad (4)$$

Where  $u^*$  is weighting function,  $q$  is the normal derivative of  $u$ ,  $q^*$  is the normal derivative of  $u^*$ ,  $\Omega$  is the solution domain and  $N$  is the numbers of boundary element.

The equation system obtained by applying equation (4) after the substitution of the boundary conditions and separation of the unknown and known variables, is given:

$$[A]\{u\} = \{b\} \quad (5)$$

Where  $[A]$  is the coefficient matrix,  $\{u\}$  is the vector of unknown values of potential and normal electric field on the boundaries and  $\{b\}$  is an independent vector.

The principle advantage of the boundary element method is that it is capable of providing very accurate predictions of the potential and current and the mesh is required only on the boundaries of the solution domain. The normal electric potential is also obtained directly as part of the BEM solution.

The boundary element software BEASY- Corrosion and CP [12] was used to investigate the performance of CP and ICCP system design and predict the potential and current values on the structure and in the surrounding environment.

## OPTIMISATION METHODS

The design of the ICCP system is a critical process and has a significant influence on the effectiveness of the corrosion protection of for example the wetted surface of a ship. The optimum design goal is to produce an evenly distributed electric potential on the hull and major appendages as well as minimise the power consumption required.

The objective function and constraint condition was originally proposed in reference [10]:

$$\min \quad f(i, s, u, P) = \left( \sum_{k=1}^n \frac{|u_t|}{|u_t| - |u_t - u_k|} \right) - \frac{\mathbf{e}}{P(i, u, s)} \quad (6)$$

$$\text{with} \quad u_{\min} \leq u_k \leq u_{\max} \quad k = 1, \dots, n \quad (7)$$

$$\text{and} \quad x_{\min} \leq x_m \leq x_{\max} \quad m = 1, \dots, p \quad (8)$$

Where:

$P(i, u, g)$  is the electric power consumption on the anodes

$\mathbf{e}$  is a weight factor to incorporate the power consumption in the objective function

$i$  is the anode electric currents

$u$  is the potential at the measurement points

$s$  is the location of the anodes

$u_{\min}$  and  $u_{\max}$  is the minimum and maximum protection potential level on the wetted surface of the ship (set up as -0.78 to -0.88 VoltAg/AgCl respectively)

$u_k = (u_1, u_2, \dots, u_n)$  is the potential at the measurement points, which are required to satisfy the constraint  $u_{\min} \leq u_k \leq u_{\max}$

$u_1$  is the threshold potential and is defined as -0.83 VoltAg/AgCl on the reference cell

$x_m = (x_1, x_2, \dots, x_p)$  are the measurement points on the wetted surface, usually  $p \geq n$ .

The objective function provides a measurement of the uniformity of the potential distributions on the wetted surface of the ship with a particular anode arrangement.

The global optimisation algorithm proposed in this paper is “Simulated Annealing” which is a computer simulation method based on a strong analogy between the physical annealing process of solids and the problem of solving large combinatorial optimisation problem [14 - 16].

The main advantage of this approach is the substantial independence from the specific design problem. The only inputs to the optimisation method are a proper cost (objective) function whose minimisation leads to a solution of the problem, and simple “tuning” of the SA parameters in order to improve the search according to the function behaviour. The main disadvantage of method is the high computation cost due to the large number of functional evaluations (e.g., BEM solutions). The flow chart of the proposed SA algorithm is shown in Figure 1.

The actual minimum was achieved by a penalty method [11]. The expended objective function of the algorithm is defined as [10]:

$$\min_{x_i \in D} F(i, s, u, P) = f(i, s, u, P) + r \sum \frac{1}{G(i, s, u, P)} \quad (9)$$

Where  $x_1 = x_1, x_2, \dots, x_L$  are the anode locations,  $L$  is the total numbers of anodes and  $D$  is the domain of the wetted surface.  $r$  is a positive weighting coefficient that ensures that; during the optimisation the constraints  $G(i, s, u, P)$  are not violated. The effect of this function is to create an artificial minimum in the vicinity of the boundary. The constraints are defined to meet following threshold:

$$G(i, s, u, P) = \left( \sum_{k=1}^n uk - \sum_{j=1}^N u_j \right) \geq 0 \quad (10)$$

Where the second term of (10) is a defined threshold potential and  $N$  is a threshold number of measured potentials that meet  $u_{\min} \leq u_j \leq u_{\max}$  in the next trial computation,  $G(i, s, u, P)$  therefore is an overall measurement to the potential distribution of a particular anode arrangement. The optimisation behaviour relies on the choice of weighting coefficient  $r$  and the exceeded constraints. These parameters have been chosen based on the experience during the optimisation process.

## ICCP OPTIMISATION OF A SHIP

A sample ship with a length of 30 meters was investigated. The geometry of interest in the boundary element model was the wetted surface of the hull and major appendages. The ICCP system evaluated included 2 anodes and a centre controlled power supply.

In the present design, the ship has two propellers and rudders and the propellers are made of nickel-aluminium-bronze alloy (NAB) and modelled as solid disks with equivalent surface area as the real elements. The shaft is made of steel and the propellers and shafts were assumed to be uncoated because of turbulence engendered by propeller movement. The ship hull and rudders are also made of steel, which is coated to provide initial protection from corrosion.

With such a design, there is a significant risk of galvanic corrosion on the steel surface. The high water velocity and turbulent flow can accelerate the corrosion. The highly turbulent flow of seawater on the surface of propeller can cause pitting, crevice attack, erosion, cavitation damage, and corrosion fatigue. Fouling increases the localised corrosion, which is accelerated as metallic ions are leached from anti-fouling paint. As steel surfaces are coated, severe local attack can occur rapidly on any damaged surface due to the very high current density caused by the galvanic action.

The definition of the paint status, location and damaged areas in the computer model are based on observations of the same and similar class of ships in dry-dock after the ships have served a certain period of time. Paints and coatings are normally damaged on parts of the hull, especially on the aft zone around propellers.

To determine the characteristics of the damaged paint, the conductivity of old and new paint was measured and compared. Observation reveals that there are a lot of small, local bare steel areas on the damaged paint surfaces. In the present computer model, the positions of the damaged paint surface and percentage of bare steel surfaces on the damaged paint surface are a statistical representation of the observations of the real ships.

The equivalent conductivity (impedance) of the damaged paint surfaces is based on the ratio of the bare steel to that of the painted surface. The equivalent conductivity of the damaged paint surface is then modelled as a percentage of the polarisation response of steel. The perfect painted steel hull was modelled as insulated surfaces.

In the computer model for the sample ship, 15% of the paint surface on the ship hull, mostly concentrating on the aft zone around the propellers is defined as damaged paint. The conductivity of the damaged paint surfaces is defined as 10% polarisation response of the steel.

The ship is surrounded by an infinite region of seawater and was modelled by a boundary of the solution domain far away from the ship hull region of interest. The seawater was defined with a constant conductivity of 5  $s/m$  in the computer model. All elements are 9-point quadratic element. The boundary element mesh discretization of the ship consists of 821 elements and 4350 nodes.

Accuracy of the electrochemical analysis is dependent upon the material polarisation involved in the boundary element model. In this computer model, linear representation of the polarisation was used which matches the service condition. In general experimental polarisation data [13] should be used in the investigation.

The anode currents determine the potential level on the hull surface and an iterative process of adjusting the anode currents and running the BEM software obtains the required values.

As the objective of the simulated annealing algorithm is to evaluate the global minimum and distinguish the local minima, the anode position is relocated based on the computation result from SA algorithm while boundary element mesh discretization is kept unchanged. In this case, the simulated annealing algorithm was used to evaluate the objective function  $f(i, s, u, P)$  with the constraints, the minimum distance in this study was set up roughly as 1.0 meter apart and this found to be the good representative to the global map of the investigated optimisation problem.

The ship hull under evaluation comprises a 3-D profile. To reduce the degree of co-ordinate variations, a map of the ship hull is stretched into a 2-D plane around 20 meters by 4 meters. The mesh discretization was designed to represent the most likely positions that the anode will be moved to in the SA movements.

The SA algorithm was run over 4 times with initial co-ordinate  $x = (20, 3), (8, 2), (5, 3), (15, 1)$ . The global minimum was found in each case and SA algorithm stopped successfully on the global minimum irrespective of where the initial anode was located. The SA movements are about 200 for each case and the effective SA movements related the initial co-ordinates are 29, 25, 18 and 34 respectively.

The process of convergence of the normalised objective function  $f(i, s, u, P)$  when the initial co-ordinate is located at  $x = (15, 1)$  is illustrated in Fig 1. The SA algorithm moves to the promising global region and searches between local and global minima. The global minimum is found successfully where the constraints are being obeyed even if the location between the local and global minimum very closes.

The objective function oscillates in the vicinity of the global minimum location since the complexity characteristics of the geometric on the aft zone.

The final optimum location of anode and electric potential on the ship hull is illustrated in Fig 2. The electric potential of the initial anode position at  $x = (15,1)$  and final optimised location at  $x = (3,3)$  along a line on the ship hull below water line 1.25 meters and along the keel line are shown in Fig 3 to Fig 6 respectively.

The result obtained represents a more evenly distributed electric potential on the ship hull. That is one of the most significant benefits of the optimisation process. The reduction in the area of under or overprotection achieved by the optimum process enables the ICCP system to protect the ship hull from corrosion more effectively.

## **MODELING CP INTERFERENCE NEAR CHEMICAL STORAGE TANKS**

In this study the design of a CP system to protect the external surface of floors on a number of large, above ground chemical storage tanks located in close proximity to each other was investigated [18]. This problem offers a significant challenge if CP interference is to be minimized. What makes this task difficult is that, in some cases, the tank floors are uncoated. Thus large CP currents are required to fully protect the steel. The effect of this large current combined with the steel floor being located at ground level and immediately adjacent to buried pipelines and steel foundations creates the ideal situation for CP interference.

Three 56.5 m diameter tanks are positioned 28m apart (84.5 m from tank center to tank center) and aligned in a row. The external floors of all three tanks are cathodically protected using four anode groundbeds, as shown in Fig 7. Each tank was protected using its own DC power source employing a current of 80A per tank (i.e. total current 240A). The DC circuit was designed so that the two anodes protected each tank floor diametrically positioned 14m from the edge of each tank, with each anode contributing to 50% of the total current requirement for the tank. Thus, the two outer anodes carried a current of 40A each while the two inner anodes discharged a current of 80A each

The anodes were 0.2m in diameter, 10m long, and initially buried vertically so that the tops of the anodes were located 20m below the ground surface. To ensure that the CP interference was not underestimated the soil resistivity was assumed to be uniform and equal to the surface resistivity of 50-ohm m. The pipeline was located immediately above one of the inner anodes and extended in a direction away from both the tanks and the anodes. Once again, to ensure that the CP interference was not underestimated, the coating defects were located immediately above the anode and at the extremity of the pipe, i.e. 65m from the anode.

Fig 8 shows the potential distribution over the tank floor with respect to a saturated Cu/CuSO<sub>4</sub> reference electrode, It shows, as predicted, that the center of the tank receives less protection than do the tank edges. Notably potentials at the center of the tank are slightly more positive (approximately -820mv) than the ideal protection criterion of -850mV suggesting that, initially, 80A may not be sufficient to fully protect the tank. The oval shape of the contours is indicative that the anodes are positioned too close to the tanks. To achieve a more symmetrical distribution of protection the anodes would have to be buried at a greater depth

### **Cathodic Interference on the buried Pipeline**

Table 1 summarizes the effect of CP interference on the pipe as a function of the size of the coating defect. As intuition may suggest, locating the pipeline within the influence of the anodic field results in CP current being picked up by the pipeline in the vicinity of the anode and being discharged at the remote end of the pipeline. Assuming the worst-case scenario that the corrosion process involves

formation of Fe, the current densities corresponding to current discharge can be converted to metal loss per year. The severity of this interference is now readily apparent and the results suggest that it would be prudent to undertake further measures to help minimize the interference

It is interesting to note that the corrosion rate is predicted to be higher when the coating defects are smaller. This suggests that smaller coating defects tend to focus the interference effects, and thus increase the damage caused by the interference on the pipeline.

One possible measure to help minimize the interference effects is to bury the anodes at a greater depth and thereby minimize the anodic interference. Table 1. summarizes the effect of lowering the anodes so that the top of the anodes is located at a depth of 70m the model predicts that repositioning the anodes has major effect on interference levels. It not only increases the effect of CP interference but also relocates the corrosion site. Corrosion that was initially located at the remote end of the pipe is now located immediately above the groundbed. This occurs because lowering the anodes removes the anodic field at the ground level. The pipeline is now subjected only to the cathodic field of the tanks. As result current is picked up at the remote end of the pipeline and conducted along the pipeline before being discharged back into the ground at the point where the pipeline closely approaches the tank floors.

The fact that positioning the anodes at greater depths reverses the current flow induced by the CP interference suggests that there is an optimum depth at which anodes could be buried so that interference is minimized. Determining the optimum depth could be evaluated efficiently using computer modeling. This would help to minimize the number of field tests to be undertaken.

## **CONCLUSIONS**

The approach described here, using the Boundary Element Method software, provides a computationally efficient method to predict the performance of CP systems and assess the impact of electrical interference. The models are useful not only for the design of new CP systems, but also for the analysis of systems that are undergoing modifications or additions.

Using computer modeling it is possible to model CP performance and interference in a manner which is enlightening regarding the processes at work. It can provide information about the level of interference in terms of a parameter (i.e. current density) that more clearly defines the severity of the effect. Furthermore, it can provide important insight into the factors that influence the magnitude of the effect. This makes computer modeling a useful tool for the design of CP systems.

The optimisation of ICCP anode locations was performed using the boundary element method coupled with a simulated annealing algorithm and direct search. The combination has been shown to effectively solve this difficult global optimisation problem.

The SA method is computationally expensive due to the many function evaluations in the computational process. At each step the potential distribution on the ship hull has to be predicted using the BEM model. Precise adjustments to the anodes are necessary, as the potential solution is sensitive to the anode current.

Further works is ongoing to achieve lower computation cost by improving the simulated annealing method and using more effective BEM models.

## **ACKNOWLEDGEMENTS**

The chemical tank model study was developed in conjunction with Computational Mechanics Australasia and Rustic Pty. The contributions of Graham Strong and Richard Rudas are acknowledged.

The major contributions of Pei Yuan Hang of DSO Singapore to the ship model study is also acknowledged.

## REFERENCES

1. Brebbia, C. A. and Dominguez, J., *Boundary Elements: An Introductory Course*, CML Publications, Southampton, 1980
2. DeGiorgi, V. E., Thomas, E. D. and Luas, K.E., *A Combined Design Methodology for Impressed Current Cathodic Protection Systems*. *Boundary Element Technology XI*, 1996
3. R. A. Adey and Pei Yuan Hang, *Computer Simulation as an aid to Corrosion Control and Reduction*, National Association of Corrosion Engineering (NACE), conference 99, San Antonio, Texas, USA, Apr., 1999
4. G. Finoly, A. Getnay and A. Giroud, *Application and Validation of the Boundary Element Method to Cathodic Protection Designs on Vessels*. *Boundary Element Technology XIV*, 1992
5. J Simkin, C W Trowbridge, *Optimizing Electromagnetic Devices Combining Direct Search Method with Simulated Annealing*, *IEEE Trans on MAG*, Vol.28, No.2, Mar. 1992
6. G Drago, A. Manella, M. Nervi, M. Repetto and G. Secondo, *A Combined Strategy for Optimisation in Non Linear Magnetic Problems Using Simulated Annealing and Search Technology*, *IEEE Trans on MAG*, Vol.28, No.2, Mar. 1992
7. K.Preis, O. Biro, M. Friedrich, A. Cottvald and C. Magele, *Comparison of Different Optimisation Strategies in the Design of Electromagnetic Devices*, *IEEE Trans on MAG*, Vol.27, No.5, Sep. 1991
8. Hou, L.S. and Sun, W., *Numerical Methods for Optimal Control of Impressed Cathodic Protection Systems*, *Int. J. of Numerical Methods in Engrg.* Vol.37, 1994
9. Hou, L.S. and Sun, W., *Optimal Positioning of Anodes for Cathodic Protection*. *SIAM J. Control and Optimisation*, Vol.34, No3, 1994
10. Pei Yuan Hang, *Investigating ICCP system design of ship with waterjet propulsion using boundary element*, *Boundary Element Technology XIV*, 1999
11. R. Fletcher, *Practical Methods of Optimisation*, John Wiley & Sons, 1980
12. *Computational Mechanics*, BEASY-CP User Guide, Computational Mechanics BEASY, Aug. 1996
13. Harvey P. Hack, *Atlas of Polarisation Diagrams for Naval Materials in Seawater*, Carderock Division, Naval Surface Warfare Centre, Apr. 1995
14. E. Aarts and J. Korst, *Simulated Annealing and Boltzmann Machines*, John Wiley & Sons, 1989.
15. Nevio Benvenuto, Michele Marchesi and Aurelio Uneini, *Applications of Simulated Annealing for the Design of Special Digital Filter*, *IEEE Trans. on Signal Processing*, Vol.40, No.2, Feb. 1992.
16. F. Catthoor, H. De Man and J. Vandewalle, *Simulated-annealing-based Optimisation of Coefficient and Data Word-lengths in Digital Filters*, *Int. J. Circuit Theory Appl.*, Vol.16, 1988.
17. S. R. White, *Concept of Scale in Simulated Annealing*, in *Proc. IEEE ICCD'84* (New York, NY), Oct. 1984.
18. Strong, G. E, Adey R A, and Rudas R S, *Computer prediction of stray current corrosion*. Australian Corrosion Conference, Melbourne, November 1997

Depth of Anodes	Area Of Coating Defect	Current Density Adjacent to Anode	Induced Corrosion Rate Adjacent to Anode	Current Density at Remote End	Induced Corrosion Rate at the Remote End
(m)	(cm <sup>2</sup> )	(mA/m <sup>2</sup> )	(mm/year)	(mA/m <sup>2</sup> )	(mm/year)
20	500	-198	-	198	0.2
20	5	-442	-	442	0.5
70	500	969	1.1	-969	-
70	5	2370	2.7	-2370	-

*Table 1. CP Interference on the Buried Pipeline*

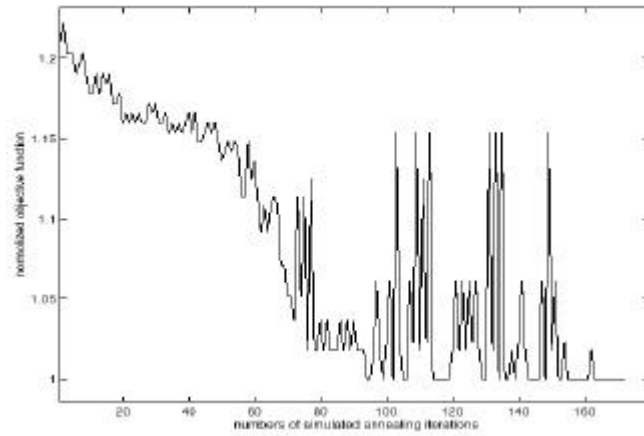


**Fig 1.** Process of convergence of normalised objective function

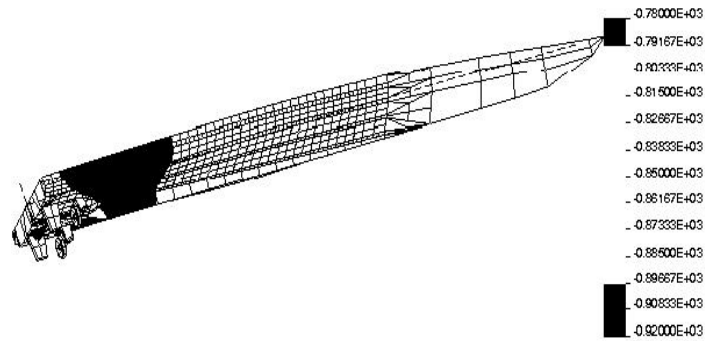


**Fig 2.** Potential distribution on the ship hull of  $x=(3,3)$

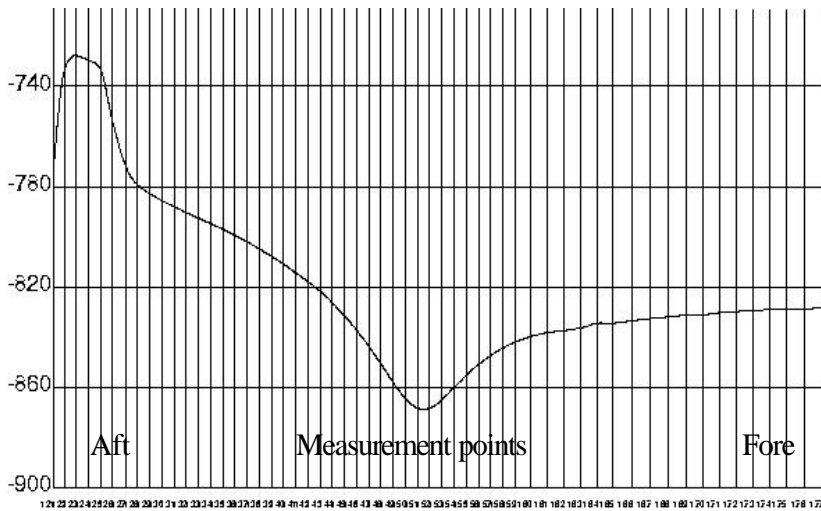


**Fig 3.** Potential distribution (mV) on the ship hull 1.32m below water line before optimisation

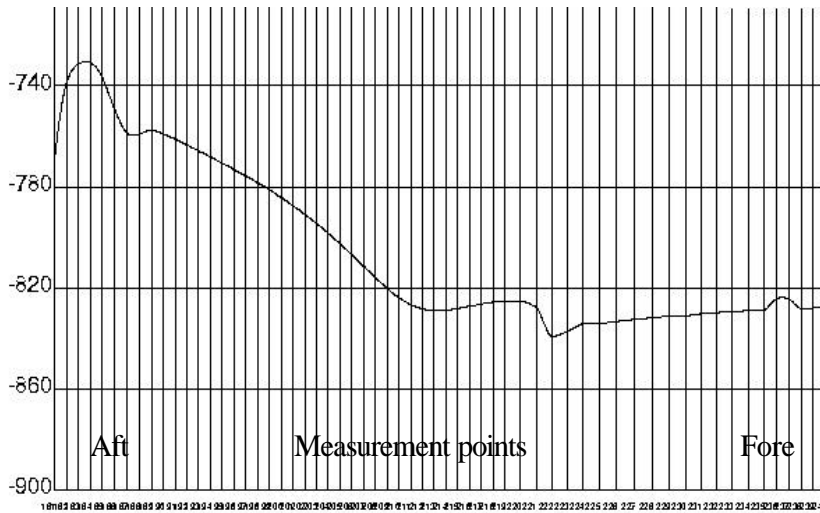


**Fig 4.** Potential distribution (mV) on the keel line of the ship hull before optimisation

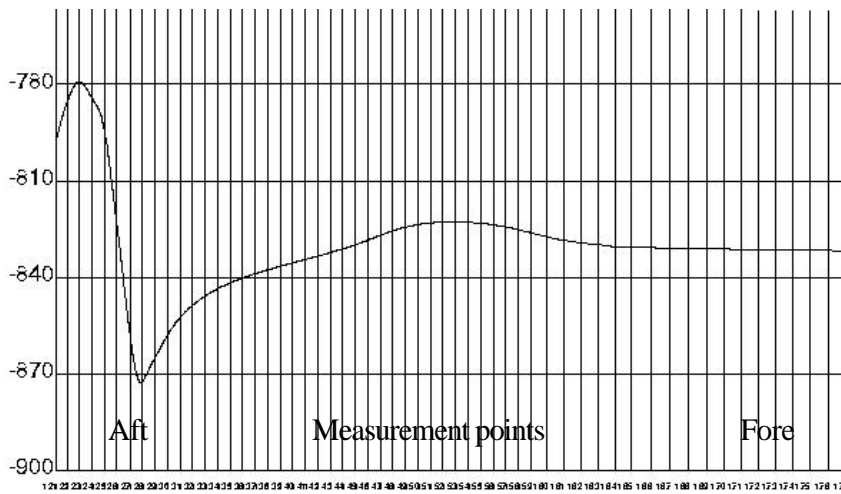


**Fig 5.** Potential distribution (mV) on the ship hull 1.32m below water line after optimisation

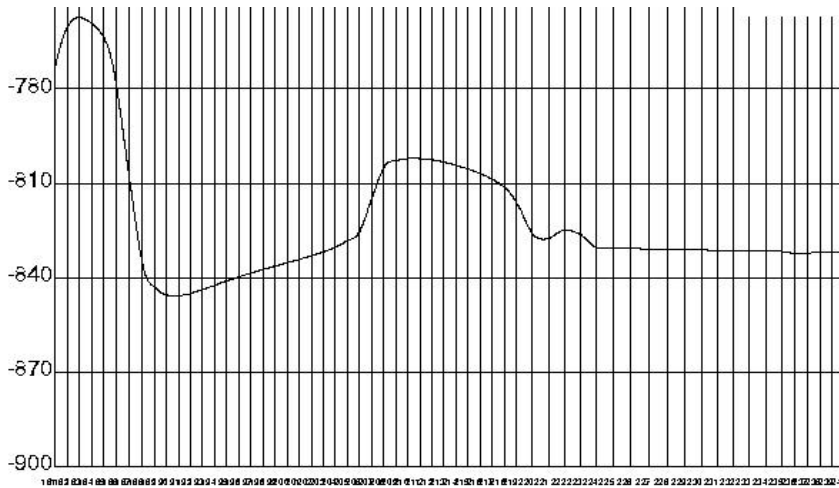


**Fig 6. Potential distribution (mV) on the keel line of the ship hull after optimisation**

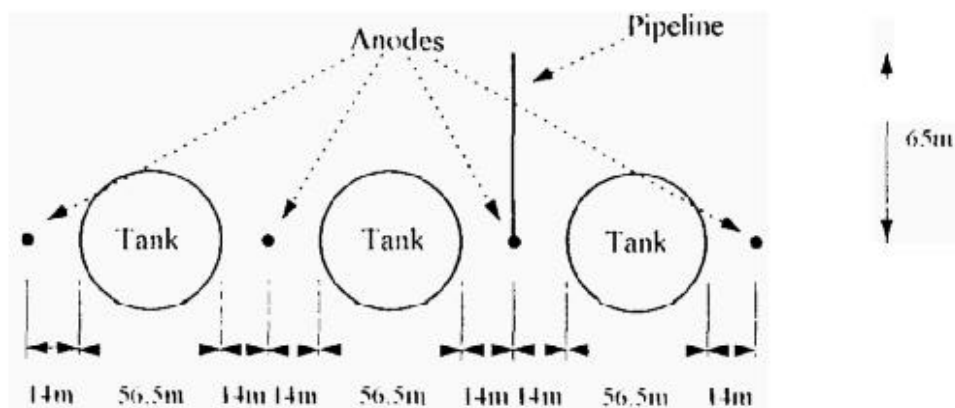


**Fig 7. Top view showing the general arrangement of the tanks, the pipeline, and the anodes. Coating defects on the pipeline were located at the extremities of the pipeline**

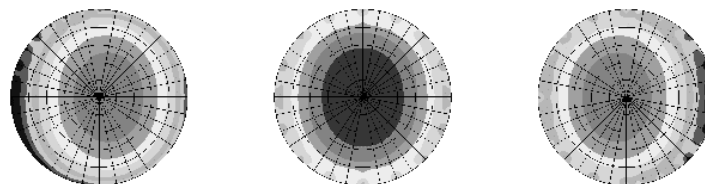


**Fig 8. Predicted Potentials on the floors of the tanks**